



ELSEVIER

Physica C 357–360 (2001) 1160–1164

PHYSICA C

www.elsevier.com/locate/physc

# Bi–Sr–Ca–Cu–O conductors and magnets at high stress–strain levels

H.W. Weijers <sup>a,\*</sup>, J.M. Yoo <sup>b</sup>, B. ten Haken <sup>c</sup>, J. Schwartz <sup>d</sup>

<sup>a</sup> National High Magnetic Field Laboratory, 1800 E. Paul Dirac Drive, Tallahassee, FL 32310, USA

<sup>b</sup> Korea Institute of Machinery and Materials, Kyungnam 641-010, South Korea

<sup>c</sup> University of Twente, Enschede 7500 AE, The Netherlands

<sup>d</sup> National High Magnetic Field Laboratory, College of Engineering, Tallahassee, FL 32310, USA

Received 16 October 2000; accepted 21 November 2000

## Abstract

We focus on a react and wind Bi-2223 conductor with a pure silver matrix. The stress–strain–critical current relation is determined for coils with a uniform stress distribution, at 4.2 K and 19 T. Somewhat surprisingly, the coils fail at a Lorentz force induced strain value close to the value for uni-axially loaded straight samples. This implies that bending strain is only partially retained due to the plastic nature of the pure silver matrix. Also, a double-pancake coil with a 15 mm winding thickness, resulting in a non-uniform stress distribution, is tested at 4.2 K and 19 T. The coil current is cycled with increasing peak values and the onset and evolution of critical current degradation in the coil is shown. © 2001 Elsevier Science B.V. All rights reserved.

*Keywords:* Bi-2223; Lorentz force

## 1. Introduction

A careful design of high-field insert magnets requires detailed knowledge of the operational limits of the superconductor and accurate models predicting the strain state of the conductor [1,2]. In this work, we focus on a react and wind Bi-2223 conductor with a pure silver matrix. The goal is to investigate how bending strain and Lorentz force-induced strain determine the onset of operating-current induced critical current degradation in insert coils. A second goal is to determine the

strain gradient, and the location and magnitude of the maximum strain within the windings. This depends on the degree to which turns are mechanically coupled.

The Bi-2223 conductor used in this study is fabricated using the PIT process, resulting in a 61-filament conductor of  $0.32 \times 4.09$  mm<sup>2</sup> cross-section with a ductile pure-Ag matrix. The heat treatment is carried out with the conductor at 0.55 m diameter. The self-field  $I_c$  ranges from 110 to 135 A at 4.2 K.

## 2. Experimental approach

All  $I_c$  measurements take place at 4.2 K in a resistive magnet at the NHMFL, which is equipped

\* Corresponding author. Tel.: +1-850-644-3102; fax: +1-850-644-0867.

E-mail address: weijers@magnet.fsu.edu (H.W. Weijers).

Table 1  
Properties of Coils A, B and C

Coil	Inner diameter (mm)	Outer diameter (mm)	Winding thickness (mm)	# turns	Height (mm)	Conductor length (m)	$I_c$ (19 T) (A)
A	97	100	1.2	6	9	1.8	36.5
B	155	158	1.2	6	9	2.9	40
C	97	128	15.4	80	8.8	28.2	35

with a 0.165 m cold-bore cryostat.  $I_c$  is determined using the  $10^{-4}$  V/m criterion.

Three coils are wound, each double pancakes from a single section of conductor and with Kapton tape of 0.033 mm thickness as insulation. Two coils, A and B, are wound with 1.2 mm winding thickness to ensure uniform stress and strain within the coils. Coil C has a 15.4 mm winding thickness resulting in significant gradients in stress and strain. Table 1 introduces the main parameters of the coils.

Manganin wires of 0.13 mm diameter are wound on the outer turns as strain gauges. This assembly is then vacuum-impregnated with Stycast 1266. The manganin wire shows a +0.49% resistance change per % strain at 4.2 K. Magneto-resistance is  $-0.273\%/T$  at 4.2 K for  $B \geq 5$  T. The self-field magneto-resistance contribution to the signal is subtracted.

At 19 T, the operating current is cycled between zero and increasingly higher peak values, until the critical current is severely degraded. The strain measured at 0 A is taken as the plastic component of the strain at the previous peak current.

### 3. Results

For *uni-axial tensile tests*, bare conductor is instrumented with a strain gauge wire over the entire length between the grips, insulated with Kapton and vacuum-impregnated with Stycast 1266, using the same process as used for the coils. At 4.2 K, the conductor can be tested to 59 MPa and 0.27% strain in the manganin wire, before yield or slipping occurs at the grips (see Fig. 1). The conductor shows significant plasticity as the residual strain is about half of the applied strain. The stress is calculated using the cross sectional

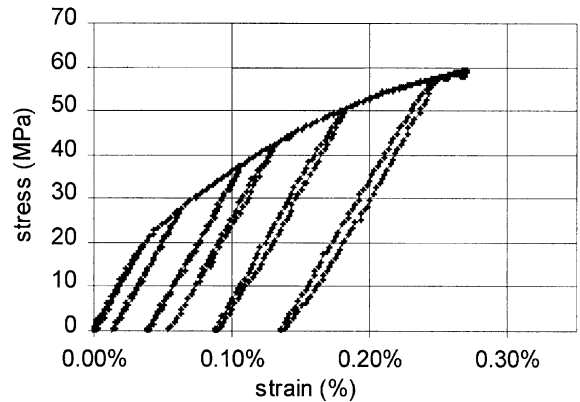


Fig. 1. The stress–strain curve of the conductor with Kapton tape and manganin wire in uni-axial tension at 4.2 K. The strain is determined using a manganin wire and is calibrated against an extensometer and the grip displacement of the tester.

area of the conductor plus insulation, and is corrected for the force on the manganin wire. We estimate that the UTS is 61 MPa at 0.28–0.29% strain for the conductor with Kapton insulation.

#### 3.1. Bending

For a perfectly elastic material with thickness  $t$ , the surface bending strain can be calculated as  $t/D$ , where  $D$  is the bending diameter. Since the thickness of the filament zone is about 0.7 times the conductor thickness, we assume that the strain on the outer filaments is 70% of the nominal surface bending strain. However, the conductor shows elastic–plastic behavior. We assume that, for deformations that do not result in significant  $I_c$  degradation, the matrix exhibits some plastic yield, thereby releasing some of the bending strain on the filaments. To quantify this, several pieces are wound to one turn at a specific smaller radius and released. About 55% of the calculated elastic

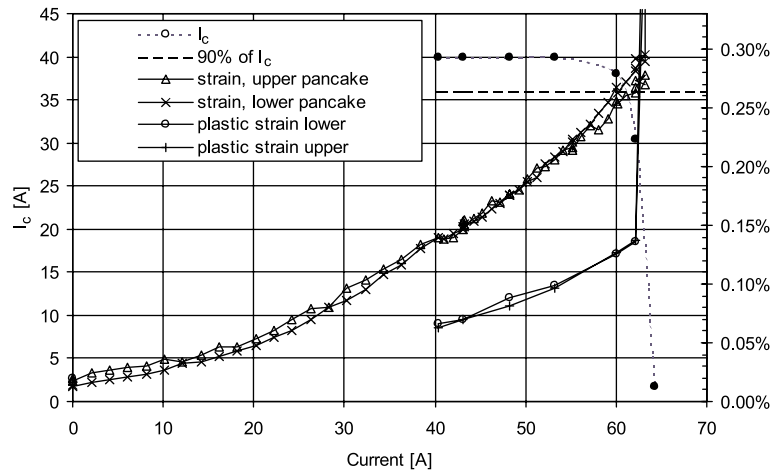


Fig. 2.  $I_c$  and strain in Coil A plotted versus the operating current. Lines between datapoints are a guide to the eye.

surface strain is released by plastic yield of the matrix, corresponding to a retained strain of 34% for the outer filaments.

*Coil A* failed at an operating current of 61 A and a measured Lorentz force induced strain of 0.26 and 0.27% for the respective pancakes. The residual strain is around 0.13%. An increase of the maximum operating current to 62 A leads to a dramatic increase in strain, including residual strain (see Fig. 2). At 61 A the average stress in the windings is 62 MPa.

*Coil B* was operated to a maximum operating current of 81 A, corresponding to a strain of 0.24%, without reaching its UTS. The residual strain after 81 A, equivalent to an average stress of 48 MPa, is 0.12%. The current leads separated from the outer turns at 77 A, when ramping towards a new peak value, terminating the experiment.

The voltage tap positions of *Coil C* are labeled A through E for both the top and bottom pancake. Voltage taps span between these positions as indicated in Table 2. Table 2 and Fig. 3 present the onset and development of degradation in Coil C as a function of the operating current at 19 T. A thermal cycle after 54 A causes a few percent  $I_c$  degradation. The subsequent slight increase in  $I_c$  for the outer sections is the result of magnetization due to the high operating current. As the Lorentz

Table 2  
Properties of Coil C

Section	Radius (mm)	$I_c$ (19 T) (A)	$I_c$ (A)
Inner (A–A)	48.8–49	26 <sup>a</sup>	47 <sup>a</sup>
AB bottom	49–52	38.2	60.5
BC bottom	52–55	36.5	67
BC top	52–55	33.3	67
CD bottom	55–58	32.9	81
CD top	55–58	39.2	80
DE bottom	58–61	35.3	86
DE top	58–61	37.3	86
Whole coil	48.6–64	35	62

<sup>a</sup> Values are lower than expected because of handling damage.

force loads increase, critical current degradation spreads from the inside to the outside of the coil, with little variations between the individual pancakes. Note that after an operating current of 90 A, all sections show an  $I_c$  of 20–25% of the starting value, but that the inner sections show a more gradual degradation. The datapoints at 71 A do not seem to follow the trend of the other datapoints. This may be related to a change in strain rate, required to prevent thermal runaway. Strain data was recorded during some of the above measurements. From the available data we observe that increasing the peak current from 85 to 90 A corresponds to an increase in residual strain of  $0.2 \pm 0.1\%$  to  $1 \pm 0.1\%$ .

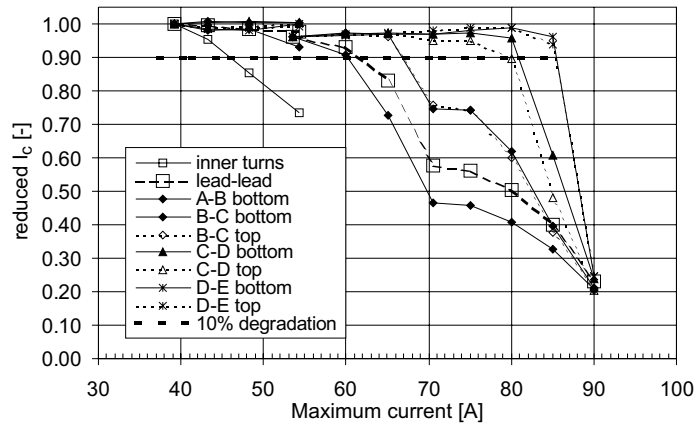


Fig. 3. Normalized  $I_{c,s}$  in sections of Coil C and the coil as a whole in a 19 T background field, versus the maximum operating current. Lines between datapoints are a guide to the eye.

#### 4. Discussion

Coils *A* and *B* are wound to radii that result in  $I_c$  degradation from 8% to 14% in short samples bend to the same radius. However, these coils sustain at least an additional 48 MPa Lorentz force-induced strain before further degradation occurred. Coil *A* fails at an average stress which is very close to the limit in uni-axial tension. The measured critical Lorentz force-induced strain in Coil *C* is 0.26–0.27%, slightly below the estimated maximum uni-axial strain of 0.28–0.29% in insulated conductor. The difference is comparable to the estimated bending strain on the outer filaments of 0.014%, but also comparable to the estimated margin or error.

Coil *B*, with an estimated maximum bending strain on the filaments of 0.08%, can be operated to a Lorentz force-induced strain of at least 0.24% and 48 MPa without overall failure and associated plastic deformation. This is a higher sustainable stress–strain level than the uni-axial limit minus the maximum bending strain. It appears that either the Lorentz force-induced strain releases some of the bending strain by plastic deformation of the matrix, or that the temperature rise associated with soldering leads to the coil anneals the conductor.

Coil *C* shows a clear pattern of  $I_c$  degradation starting at the inner turns and progressing outward with increasing load. This is consistent with turns

that are mechanically coupled and can be considered, in first approximation, as mechanically isotropic [3]. The independent turn, or JBR model, predicts the location of highest strain in the outer turns, also when considering bending strain, and is therefore not correct. A generalized plane strain model is expected to be more suitable to predict the stress–strain state [4]. As the inner sections reach their UTS, any further increase in load is carried by the next section outward, limiting the yield and  $I_c$  degradation of the inner section. There is no such support for the outer sections, explaining the sharp  $I_c$  degradation and large plastic yield when the critical strain is reached.

#### 5. Conclusion

A study is presented on influence of bending, uni-axial tension and Lorentz force-induced strain on the properties of a react and wind Bi-2223/Ag conductor. In bending, the conductor shows elastic–plastic behavior, which reduces the maximum strain on the filaments to about 34% of the elastic surface strain. Two thin insert coils with a winding radius that causes about 10% bending strain degradation, sustain at least 48 MPa Lorentz force and 0.24% induced strain before further  $I_c$  degradation occurs. A coil with 15 mm radial build degrades from the inner radius outward with

increasing load. This is consistent with mechanically coupled turns.

### **Acknowledgements**

Research supported in part by the NSF and the State of Florida under cooperative grant DMR 9527035. We thank Hans van Eck and Youri Viouchkov for technical support.

### **References**

- [1] M.U.K. Ohkura, K. Sato, T. Kiyoshi, H. Kitaguchi, H. Wada, *Adv. Supercond.* XI (1999) 995–998.
- [2] H.W. Weijers, Q.Y. Hu, Y.S. Hascicek, A. Godeke, Y. Viouchkov, E. Celik, J. Schwartz, K. Marken, J. Parrell, *IEEE Trans. Appl. Supercond.* 9 (1999) 563–566.
- [3] H.W. Weijers, unpublished.
- [4] W.D. Markiewicz, I.R. Dixon, *J. Appl. Phys.* 86 (1999) 7039–7051.